LCLS-TN-99-4
May 4,1999

Electron Trajectory in an Undulator with Dipole Field and BPM Errors

Paul Emma

SLAC

ABSTRACT

A statistical analysis of a corrected electron trajectory through a planar undulator is presented. The undulator is composed of multiple modular sections each containing *N* dipoles with random field strength errors and misaligned beam position monitors (BPMs) between each section. An analytical formula for the rms trajectory is derived to aid in the understanding of the impacts of BPM location and alignment on the trajectory. The results are applied to the LCLS FEL undulator where the requirements on electron trajectory straightness are very demanding.

1 Introduction

The requirements on the degree of straightness of an electron trajectory through an FEL undulator can be quite demanding. In order to maintain good photon/electron overlap, the trajectory must not deviate from a straight line, over a gain length, by more than a fraction of the rms electron beam size. For the LCLS FEL undulator [1] the rms beam size is ~30 μm and the straightness requirements are of the order of 5 μm over the 10-meter gain length. This trajectory straightness is achieved through tight quality control during undulator fabrication and beam steering techniques during operations. Since the location and number of beam position monitors (BPMs) along the undulator is an important factor in achieving a straight trajectory, it is useful to have a simple way in which to estimate the expected rms trajectory as a function of BPM separation distance, BPM resolution and/or alignment quality, and dipole field errors.

We derive an analytical formula which can be used to estimate the expected value of the rms electron trajectory anywhere along a simple planar undulator after steering using misaligned BPMs. Misaligned quadrupole magnets can also affect the trajectory, but steering corrections applied at or very near the quadrupoles can be used to completely compensate this component of the trajectory. Since the limit of this compensation is solely dependent on the resolution and transverse alignment of the BPMs, we can ignore quadrupole misalignments. They are implicitly included here in the steering corrections and the treatment of the BPM limitations.

2 Trajectory Analysis

A simple undulator section is shown schematically below in Figure 1. The full undulator will be composed of multiple such sections.

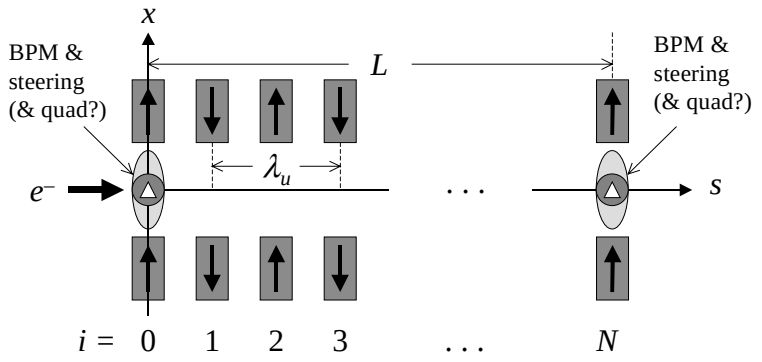

Figure 1. Simplified undulator section used to analyze the electron trajectory. The section has a length L with $N/2$ undulator periods and a BPM and steering corrector placed between each section. Quadrupole magnets may only exist at or near the BPMs. Their effects are implicitly addressed here.

The section length is given by L, the undulator period is λ_u, and there are $N/2 = L/\lambda_u$ periods over the section (N dipoles). A BPM and a dipole steering element are placed between each section. Note, a moveable quadrupole is also a steering element. For simplicity, this model includes no period breaks at the BPMs and the details of dispersion termination at the start and end of a section are ignored. Quadrupole magnets, if used, are assumed to be placed at or near the BPMs but are not addressed here since their misalignments simply change the steering corrections required and the focusing is not relevant for the single particle trajectory. The effect of an incoming betatron oscillation is also ignored since it can be removed at the undulator input with upstream steering or added later to these results as an independent effect.

A perfect undulator section (and a perfect initial trajectory) will produce a nominal *reference trajectory* which is composed of the small transverse oscillations normally associated with an undulator. This reference trajectory is subtracted off and only the difference orbit produced by small dipole field errors and steering using inaccurate BPMs is examined. For illustration purposes Figure 2 shows an LCLS example e^- difference trajectory through ten adjacent sections with N (= 128) random dipole errors per section. The trajectory has been steered exactly to zero at each section border. The initial position and angle at $s/L = 0$ are also zero.

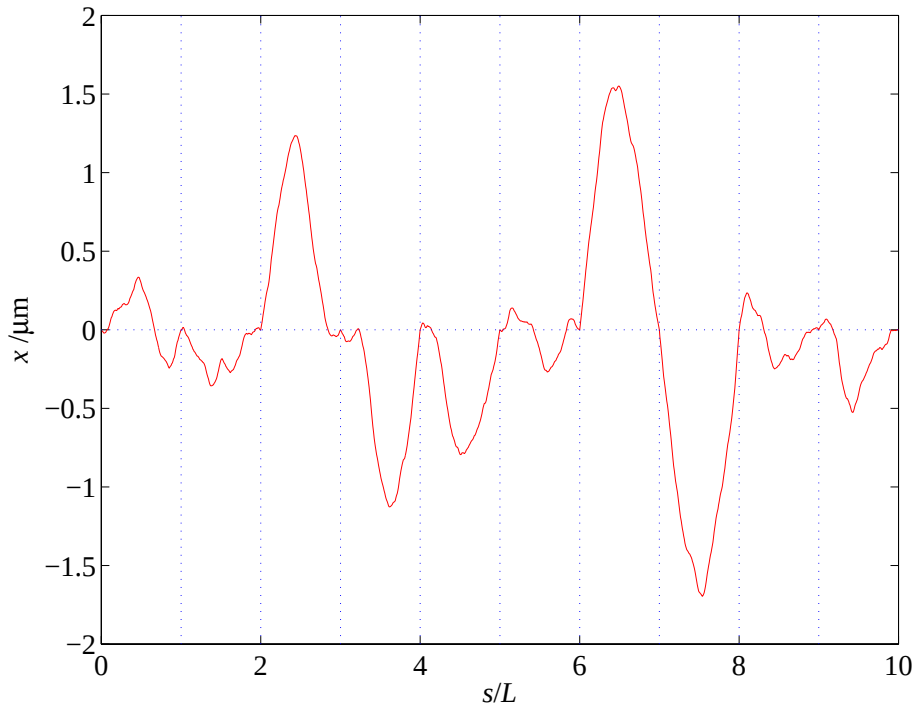

Figure 2. Example steered trajectory through ten adjacent LCLS undulator sections with random dipole errors. The trajectory has been steered exactly to zero at each section border (s/L = 1,2,…,10).

There are N (= 128) dipoles per section with rms relative errors of $\langle(\Delta B/B_0)^2\rangle^{1/2}$ = 0.1%, the undulator period is λ_u = 3 cm, the nominal peak field is B_0 = 13.2 kG, and the electron energy is 14.35 GeV. In this simple example no BPM errors are included yet. The resulting trajectory is a bounded random walk which is clamped to zero periodically.

A useful way to statistically describe this trajectory is with its rms as a function of location along one section over an ensemble of such sections. Since the full undulator is composed of many similar sections, this rms also describes the rms trajectory along the full undulator.

For a sinusoidal varying field with peak field B_0 and relative field error ($\Delta B_j/B_0$), each dipole produces an additional e^- transverse kick at the center of the dipole of

$$\theta_j = \frac{B_0 \lambda_u}{\pi(B\rho)}\left(\Delta B_j / B_0\right), \tag{1}$$

where ($B\rho$) is the standard, energy dependent magnetic rigidity. Ignoring the weak focusing of the undulator fields, each upstream kick at location j ($0 \le j < N$) displaces the electron beam at a downstream location i ($j < i \le N$) by $\Delta x_{ij} = \theta_j(s_i - s_j) = \lambda_u\theta_j(i - j)/2$. The sum over all upstream displacements, Δx_{ij}; plus the displacement, $\theta_c\lambda_u i/2$, produced by an initial beam angle, θ_c; plus an initial BPM-limited position, b_1, produces a trajectory at location i of

$$x_i = \frac{\lambda_u}{2}\left[\theta_c i + \sum_{j=0}^{i}\theta_j(i-j)\right] + b_1 \ . \tag{2}$$

The angle θ_c (at j = 0) is the sum of 1) an incoming angle from the previous section plus 2) a correction angle used to steer the trajectory to the next BPM (at section's end). The offset b_1 is the initial e^- beam position at j = 0 resulting from upstream steering of the trajectory to the first BPM offset, b_1. The BPM offset, b_1, can be interpreted as a transverse alignment error of the BPM, an electronic noise component of the BPM reading, or both combined.

The angle, θ_c, is now defined by steering the trajectory so that the next BPM 'reads' zero. Since this next BPM has a different offset, b_2, than the first BPM, the steering correction will produce $x_N = b_2$. Using Eq. (2) with $i = N$ and $x_N = b_2$, and solving for the angle produces

$$\theta_c = \frac{1}{N}\left\{\frac{2}{\lambda_u}(b_2 - b_1) - \sum_{j=0}^{N}\theta_j(N-j)\right\} \ . \tag{3}$$

Eq. (3) is now substituted into (2) and the steered trajectory at any location, i, is given by

$$x_i = \frac{\lambda_u}{2}\left[\frac{2i}{N\lambda_u}(b_2 - b_1) - \frac{i}{N}\sum_{j=0}^{N}\theta_j(N-j) + \sum_{j=0}^{i}\theta_j(i-j)\right] + b_1 . \qquad (4)$$

We now move toward a statistical analysis of the trajectory and therefore consider b_1, b_2, and the set of angles θ_j as random, uncorrelated variables. After some rearrangement Eq. (4) can be put into a form where one sum extends from $j = 0$ to $i - 1$, and a second extends from $j = i$ to N.

$$x_i = \frac{\lambda_u}{2N}\left[(i-N)\sum_{j=0}^{i-1} j\theta_j \; - i\sum_{j=i}^{N}\theta_j(N-j)\right] + \left(1 - \frac{i}{N}\right)b_1 + \frac{i}{N}b_2 . \qquad (5)$$

This form is convenient since it is a linear combination of uncorrelated, random variables and its variance, $\langle x^2 \rangle$, is simply the sum in quadrature of the components. The variance, or the expectation value of the square of the electron trajectory over an ensemble of sections, is then written as

$$\left\langle x_i^2 \right\rangle = \frac{\lambda_u^2}{4N^2}\left\langle \theta^2 \right\rangle\left[(i-N)^2 \sum_{j=0}^{i-1} j^2 \; + i^2 \sum_{j=i}^{N}(N-j)^2\right] + \frac{1}{N^2}\left\langle b^2 \right\rangle\left[(N-i)^2 + i^2\right], \qquad (6)$$

where we have used the following relations for the random, uncorrelated dipole and BPM errors (l = 1,2).

$$\left\langle \theta_j^2 \right\rangle = \left\langle \theta_k^2 \right\rangle \equiv \left\langle \theta^2 \right\rangle, \quad \left\langle b_1^2 \right\rangle = \left\langle b_2^2 \right\rangle \equiv \left\langle b^2 \right\rangle, \quad \left\langle \theta_j \theta_k \right\rangle = \langle b_1 b_2 \rangle = \left\langle \theta_j b_l \right\rangle = 0 \qquad (7)$$

The rms of the kick angles is related to the rms relative dipole errors, $\langle (\Delta B/B_0)^2 \rangle^{1/2}$, by

$$\left\langle \theta^2 \right\rangle^{1/2} = \frac{|B_0|\lambda_u}{\pi(B\rho)}\left\langle (\Delta B/B_0)^2 \right\rangle^{1/2} \qquad (8)$$

which is 0.263 μrad for the LCLS parameters. Eq. (6) is now reduced to a polynomial in i by applying the summation relations

$$\sum_{j=0}^{n} j = \frac{1}{2}n(n+1), \qquad \sum_{j=0}^{n} j^2 = \frac{1}{6}n(n+1)(2n+1) . \qquad (9)$$

$$\left\langle x_i^2 \right\rangle = \frac{\lambda_u^2}{24N}\left\langle \theta^2 \right\rangle i\left[2i^3 - 4Ni^2 + (2N^2 - 1)i + N\right] + \frac{1}{N^2}\left\langle b^2 \right\rangle\left[2i^2 - 2Ni + N^2\right], \qquad (10)$$

The index, i, is now replaced by the longitudinal axis, s (= $i\lambda_u/2$), along the undulator section, and the number of dipoles, N (= $2L/\lambda_u$), is replaced by the length of the section. In addition, with zero-mean errors (*i.e.* $\langle \theta \rangle = \langle b \rangle = 0$) the rms trajectory is simply: $x_{rms} = \langle x^2 \rangle^{1/2}$ and Eq. (10) becomes

$$x_{rms}^2(s) = \left\langle \theta^2 \right\rangle \frac{L^3}{12\lambda_u}(s/L)\left[8(s/L)^3 - 16(s/L)^2 + \left(8 - \lambda_u^2/L^2\right)(s/L) + \lambda_u^2/L^2\right] + \left\langle b^2 \right\rangle \left[2(s/L)^2 - 2(s/L) + 1\right] \tag{11}$$

For an undulator section with many dipole periods (*i.e.* $\lambda_u/L << 1$), the rms trajectory, Eq. (11), along a section ($0 \le s \le L$) simplifies to

$$x_{rms}(s) \cong \sqrt{\left[\frac{2}{3}\frac{L^3}{\lambda_u}\left\langle \theta^2 \right\rangle (s/L)^2 + \left\langle b^2 \right\rangle\right]\{1 - s/L\}^2 + \left\langle b^2 \right\rangle (s/L)^2} \ . \tag{12}$$

The mid-section value of the rms trajectory, $\hat{x}_{rms}$, is taken at $s = L/2$ and is given by

$$\hat{x}_{rms} \cong \frac{1}{2}\sqrt{\frac{L^3}{6\lambda_u}\left\langle \theta^2 \right\rangle + 2\left\langle b^2 \right\rangle} \ . \tag{13}$$

The rms trajectory in Eq. (12) is a function of *s* since the rms is taken over an ensemble of undulator sections rather than over *s*. We can also integrate out the *s*-dependence by calculating the rms of Eq. (12) over the entire section. This produces a single global rms value for the entire undulator trajectory integrated over both *s* and many random seeds. The global rms value is given by integrating the square of Eq. (12) over the section length.

$$\left\langle x_{rms}^2 \right\rangle_s^{1/2} \equiv \sqrt{\frac{1}{L}\int_0^L x_{rms}^2 ds} \cong \sqrt{\frac{L^3}{45\lambda_u}\left\langle \theta^2 \right\rangle + \frac{2}{3}\left\langle b^2 \right\rangle} \ . \tag{14}$$

Eq. (12) is compared in Figure 3 with computer generated trajectories using 1000 random seeds and for various values of $\langle b^2 \rangle$ as indicated in the figure. The simulations propagate the beam trajectory continuously through 1000 consecutive undulator sections ignoring the field gradient, but otherwise using an accurate model. Eq. (12) is shown as a dashed curve in each plot and the rms over 1000 steered sections is shown as a solid curve. To compare with the *s*-dependence of Eq. (12) the simulated trajectory is sampled at a fixed location (*s*/*L*) in each undulator section and the rms is taken for every discrete value of *s*/*L*. Since $\lambda_u/L \approx 0.02$ (<< 1), the results of Eq. (11) and (12) are virtually identical and agree well with the time consuming computer calculations. The computer calculated values of the global rms (rms over the entire 1000-section simulated trajectory) are also shown at the top of each plot. These values each agree with Eq. (14) to within <2%.

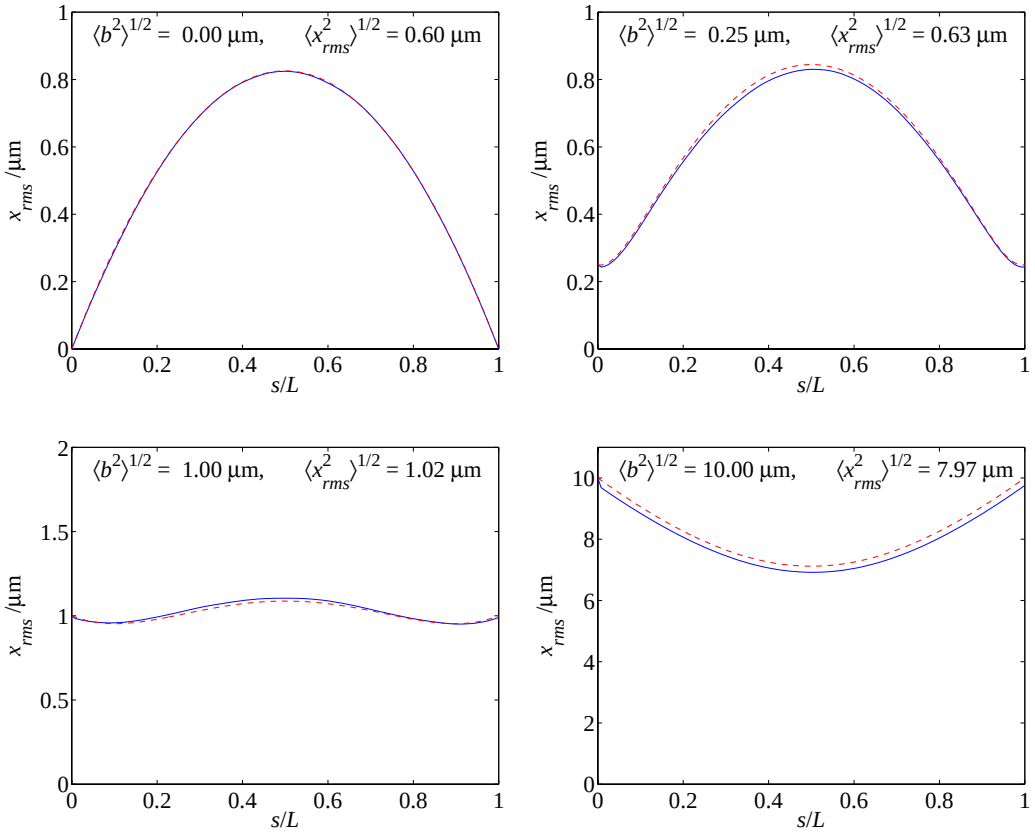

Figure 3. Trajectory rms over an undulator section showing the analytical result of Eq. (12) (dashed) and a computer calculation over 1000 random seeds (solid). The four figures are for four different values of rms BPM errors, $\langle b^2\rangle^{1/2}$ (= 0, 0.25, 1 and 10 μm), as shown on plots and λ_u = 3 cm, L = 1.92 m, B_0 = 13.2 kG, $\langle(\Delta B/B_0)^2\rangle^{1/2}$ = 0.1%, and $(B\rho)$ = (14.35 GeV)(33.3 kG-m/GeV).

3 Discussion

Eq. (14) demonstrates the somewhat obvious fact that the trajectory can be dominated by large BPM misalignments after applying one-to-one steering. That is, for misaligned (or poor resolution) BPMs of

$$\left\langle b^2\right\rangle^{1/2} > \frac{\sqrt{L^3\lambda_u}}{\pi\sqrt{30}}\frac{\Delta B_{rms}}{(B\rho)}, \tag{15}$$

the trajectory is BPM-dominated and the relative dipole errors play a less important role. In this case the rms of the trajectory simplifies to

$$\left\langle x_{rms}^2\right\rangle_s^{1/2} \approx \sqrt{\frac{2}{3}}\left\langle b^2\right\rangle^{1/2}. \tag{16}$$

For the LCLS, Eq. (15) evaluates to ~0.74 μm at 14.35 GeV and 0.1 % rms relative dipole errors which means that a 1-μm resolution BPM, even if it is perfectly aligned, will still dominate the trajectory.

The LCLS undulator trajectory will, however, be controlled using a beam-based alignment algorithm [2]. The net effect of this method, not including systematic errors, is to determine the BPM misalignments to the level of their precision (~1 μm). After the BPMs have been aligned to a level of $\sqrt{2}$ μm, Eq. (16) then suggests a final trajectory of 1.2 μm rms, which is fully adequate. The results of the beam based alignment method are, however, better left to the details of the simulations described in reference 2.

Alternate steering methods besides a one-to-one algorithm, may also be applied which may change these results. A weighted steering, where the BPMs are only zeroed to within some reasonable band and the required corrector strengths are simultaneously minimized using some prescribed weight, can generally produce a better trajectory if the weights are chosen judiciously based on some rough knowledge of the initial rms misalignments.

Finally, knowledge of the rms trajectory amplitude is not enough to fully evaluate the FEL performance. The frequency content of the trajectory with respect to the gain length may also be an important characteristic which is not studied here.

4 Conclusions

The expected rms value of a one-to-one steered electron trajectory through a planar undulator which includes BPM errors and dipole field errors can be accurately estimated using Eq. (14). The analysis presented here allows a quick estimation of the steered trajectory without using time consuming computer simulations. The method has been simplified by assuming each section has a steering corrector and BPM, and the only quadrupole fields are at or very near the BPMs. The quadrupoles may be misaligned without changing these results. The misalignments only increase the correction strengths required. A more complicated undulator structure with super-periodicity, such as multiple quadrupoles between each BPM, is not addressed here, but could be analyzed with a modified treatment. Other trajectory effects such as an incoming betatron oscillation, the Earth's magnetic field, or focusing effects within the dipole structure are also not addressed. An incoming oscillation can easily be added to these results as an additional trajectory component.

5 Acknowledgements

I would like to thank Ilan Ben-Zvi for encouraging this work and Heinz-Dieter Nuhn for a very careful reading of the draft with several important comments and corrections.

6 References

[1] *LCLS Design Study Report*, SLAC-R-521, (1998).

[2] P. Emma, R. Carr, H.-D. Nuhn, *Beam Based Alignment For The LCLS FEL Undulator*, Proceedings of the 1998 Free Electron Laser Conference, Newport News, Virginia, August 1998.